CORA Cork Open Research Archive
Cartlann Taighde Oscailte Chorcaí

Title	Electron band alignment between (100)InP and atomic-layer deposited Al2O3
Authors	Chou, Hsing-Yi;Afanas'ev, V. V.;Stesmans, A.;Lin, H. C.;Hurley, Paul K.;Newcomb, Simon B.
Publication date	2010
Original Citation	Chou, H.-Y., Afanas'ev, V. V., Stesmans, A., Lin, H. C., Hurley, P. K. and Newcomb, S. B. (2010) 'Electron band alignment between (100)InP and atomic-layer deposited Al2O3', Applied Physics Letters, 97(13), pp. 132112. doi: 10.1063/1.3496039
Type of publication	Article (peer-reviewed)
Link to publisher's version	http://aip.scitation.org/doi/abs/10.1063/1.3496039 - 10.1063/1.3496039
Rights	© 2010 American Institute of Physics.This article may be downloaded for personal use only. Any other use requires prior permission of the author and AIP Publishing. The following article appeared in Chou, H.-Y., Afanas'ev, V. V., Stesmans, A., Lin, H. C., Hurley, P. K. and Newcomb, S. B. (2010) 'Electron band alignment between (100)InP and atomic-layer deposited Al2O3', Applied Physics Letters, 97(13), pp. 132112 and may be found at http://aip.scitation.org/doi/abs/10.1063/1.3496039
Download date	2026-11-07 13:02:35
Item downloaded from	https://hdl.handle.net/10468/4330

UCC
University College Cork, Ireland
Coláiste na hOllscoile Corcaigh

Electron band alignment between (100)InP and atomic-layer deposited Al_2O_3

Hsing-Yi Chou' , V. V. Afanas'ev, A. Stesmans, H. C. Lin, P. K. Hurley, and S. B. Newcomb

Citation: Appl. Phys. Lett. **97**, 132112 (2010); doi: 10.1063/1.3496039
View online: http://dx.doi.org/10.1063/1.3496039
View Table of Contents: http://aip.scitation.org/toc/apl/97/13
Published by the American Institute of Physics



Electron band alignment between (100)InP and atomic-layer deposited Al_2O_3

Hsing-Yi Chou,[1,a)] V. V. Afanas'ev,[1] A. Stesmans,[1] H. C. Lin,[2] P. K. Hurley,[3] and S. B. Newcomb[4]
[1]*Department of Physics, University of Leuven, Celestijnenlaan 200D, B-3001 Leuven, Belgium*
[2]*IMEC, 75 Kapeldreef, B-3001 Leuven, Belgium*
[3]*Tyndall National Institute, University College Cork, Lee Maltings, Prospect Row, Cork, Ireland*
[4]*Glebe Scientific Ltd., Newport, Tipperary, Ireland*

(Received 9 August 2010; accepted 12 September 2010; published online 30 September 2010)

Energy barriers at interfaces of (100)InP with atomic-layer deposited Al_2O_3 are determined using internal photoemission of electrons. The barrier height between the top of the InP valence band and bottom of the alumina conduction band is found to be 4.05 ± 0.10 eV corresponding to a conduction band offset of 2.7 eV. An interlayer associated with the oxidation of InP may result in a lower barrier for electron injection potentially leading to charge instability of the insulating stack. A wide-gap P-rich interlayer has a potential to reduce this degrading effect as compared to In-rich oxides. © *2010 American Institute of Physics*. [doi:10.1063/1.3496039]

Like other $A_{III}B_V$ semiconductors InP attracts considerable attention as possible high-mobility channel material for next generations metal-insulator-semiconductor (MIS) electronic and optoelectronic devices. Recently, MIS transistors employing InP and the atomic-layer-deposition (ALD) grown Al_2O_3 as gate insulator have been demonstrated.[1–4] However, InP devices were reported to suffer from the threshold voltage instability[2] caused by charge injection and trapping in the insulator. This issue naturally brings band alignment at the InP/Al_2O_3 interface to attention of an experimentalist. Moreover, reliable knowledge of band alignment is needed for proper engineering of more complex stacks that use InP as a barrier layer on top of the $In_xGa_{1-x}As$ in quantum well channel structures.[3,4] In the present work we determine the electron band alignment between (100)InP and ALD Al_2O_3 using internal photoemission (IPE) of electrons. In particular, it is found that oxidation of the InP surface results in formation of a P-rich wide gap interlayer (IL), quite in contrast to the earlier studied interfaces of arsenides with Al_2O_3 exhibiting a narrow gap IL.[5–8] This finding makes the InP/Al_2O_3 interface particularly promising for application in MIS devices.

Studied samples were prepared on single crystal (100) InP of n-type (S-doped) or p-type (Zn-doped) conductivity with doping concentration of about 4×10^{17} cm^{-3}. Three predeposition surface treatments were compared: wet etch in HCl (0.1% water solution), the same etch followed by treatment in $(NH_4)_2S$ from a 25% polysulfide water solution, and UV/O_3 oxidation. Next, a layer of Al_2O_3 (8 nm target thickness) was deposited by ALD at 300 °C using $Al(CH_3)_3$ (the first pulse) and H_2O precursors. Transmission electron microscopy (TEM) cross-sectional images show almost no contrast between the IL and the Al_2O_3 layer. Nevertheless, the IL can be visualized (Fig. 1) after prolonged sample exposure to an electron beam causing alumina to crystallize, while the IL remains amorphous. In this way the thickness of the IL, which appears to be sensitive to the preclean, can be determined. The low contrast between Al_2O_3 and the IL indicates the latter oxide to be P-rich as the electron scattering amplitude increases with atomic number (Z) as $Z^{3/2}$.[9,10] Thus, a weak contrast between the oxides of Al (Z=13) and P (Z=15) is expected, while the absence of the contrast associated with In (Z=49) suggests that most of the In is probably removed during ALD.

For IPE measurements, MIS capacitors were prepared by evaporation of semitransparent (13-nm thick) Au or Al electrodes of 0.5 mm^2 area onto Al_2O_3. The IPE together with photoconductivity (PC) measurements were performed at room temperature in the photon energy ($h\nu$) range 2.0–6.8 eV. The quantum yield (Y) was determined by normalizing the measured photocurrent to the incident photon flux.[11] An example of the yield spectral curves is shown in Fig. 2 for the n-type InP/Al_2O_3/Au sample with HCl predeposition clean. Spectra measured under positive bias (open symbols) show field-independent features at E_0'=4.7 eV and E_2=5.1 eV, coinciding in energy with the excitation of direct optical transitions between high-symmetry points in the Brillouin zone of InP, i.e., $\Gamma_8^V \rightarrow \Gamma_7^C$ and $X_5^V \rightarrow X_3^C$, respectively.[12] This observation leaves little doubt that the photocurrent ob-

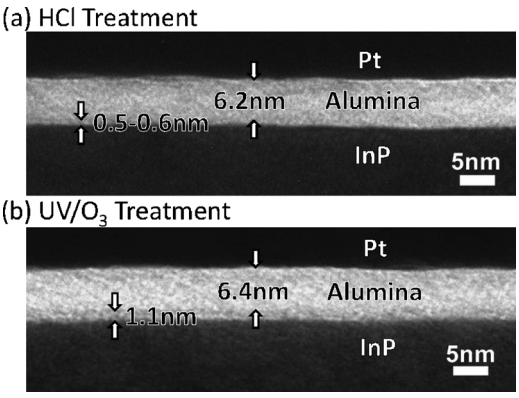


FIG. 1. Cross-sectional TEM images of the InP/Al_2O_3 interface in samples prepared using HCl treatment (a) and UV/O_3 oxidation (b) prior to ALD. The arrows mark the thicknesses of the Al_2O_3 layer and the IL grown between Al_2O_3 and InP, observed after crystallizing alumina by an electron beam.

a)Electronic mail: hsingyi.chou@fys.kuleuven.be.

 © 2010 American Institute of Physics

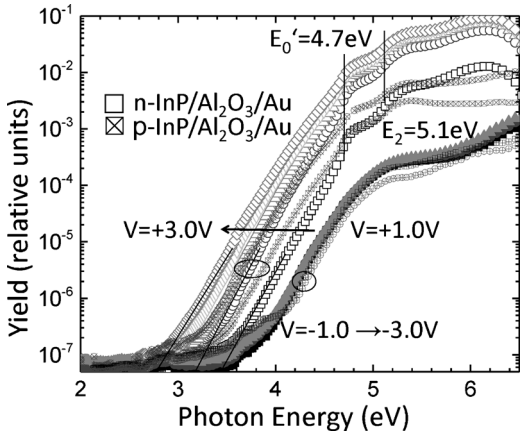


FIG. 2. IPE and PC yield as a function of photon energy measured on InP/Al_2O_3/Au samples, prepared using pre-ALD HCL etching, with the applied bias varying from 1.0 to 3.0 V (open symbols) and from −1.0 to −3.0 V (filled symbols). Vertical lines indicate energies of direct optical transitions within the InP crystal.

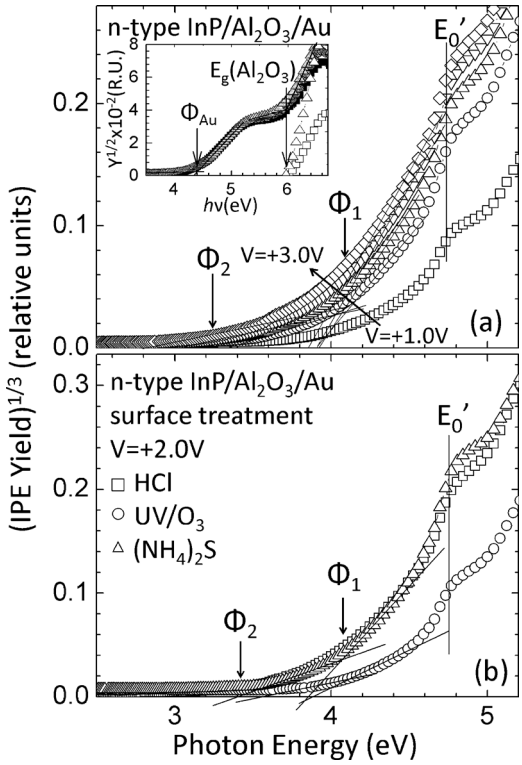


FIG. 3. (a) Determination of the IPE spectral thresholds in the pre-ALD HCl-treated n-InP/Al_2O_3/Au sample from the spectra shown in Fig. 2 using $Y^{1/3}$-hν (Powell) plots. Vertical arrows indicate the inferred spectral thresholds. The inset illustrates determination of the electron IPE threshold from Au into Al_2O_3 (Φ_{Au}) and the oxide band gap [$E_g(Al_2O_3)$] using the $Y^{1/2}$-hν plot; (b) Comparison of the IPE spectra between samples prepared using three different InP surface treatments. All curves are measured under +2 V bias applied to Au electrode.

served in the spectral range hν=3.5–5.5 eV is due to IPE of electrons from the InP valence band (VB) into the oxide conduction band (CB). By contrast, no optical signatures of InP are seen in the spectra taken under negative bias (filled symbols) suggesting electron IPE from Au into Al_2O_3. Indeed, replacement of Au with Al shifts the spectral threshold by ≈1 eV to lower hν (spectra not shown). At hν>6 eV the photocurrent spectra for both orientations of the electric field reveal the onset of intrinsic PC in alumina with spectral threshold at $E_g(Al_2O_3)=6.1\pm0.1$ eV (cf. insert in Fig. 3) in agreement with results for ALD Al_2O_3/Si.[13] Noteworthy is that in the UV/O_3 oxidized (prior to ALD) sample with the thickest IL a second PC threshold is found at 6.5±0.1 eV apparently corresponding to band-to-band excitation within the IL.

To determine the IPE spectral thresholds from the data shown in Fig. 2 for the HCl-treated n-InP/Al_2O_3/Au sample, we plotted in Fig. 3(a) the yield in $Y^{1/3}$-hν (IPE from InP) or $Y^{1/2}$-hν (IPE from Au and Al) coordinates as suggested by Powell.[14] The IPE from Au [inset in Fig. 3(a)] obeys the Fowler law yielding a threshold of $\Phi_{Au}=4.1$ eV, in good agreement with the value found in (100)Si/Al_2O_3/Au structures.[13] By contrast, the IPE spectra from the VB of InP cannot be described by a single threshold value. From the part of the curve measured in the range 3.8<hν<4.5 eV one can still find the threshold Φ_1, similar to Φ_{Au}, but the origin of the low-energy "tail" stretching down to almost 3 eV and the corresponding threshold Φ_2 is not evident. To shed some light on the source of the photocurrent in the range 3.2<hν<4 eV, we compare in Fig. 3(b) the $Y^{1/3}$-hν plots of n-InP/Al_2O_3 samples prepared using different predeposition surface treatments. Samples with HCl (□) and HCl+$(NH_4)_2S$ (△) preclean show very similar spectra, while in the sample subjected to UV/O_3 oxidation (○) the IPE is significantly attenuated. This attenuation correlates with the thicker IL (Fig. 1) suggesting scattering of excited electrons inside the IL as the major yield reduction mechanism. To be noted is that the IPE yield is reduced by the thicker IL over the whole photon energy range covered, indicating InP as the common source of photoelectrons. Further insight on the unusual behavior of the IPE from InP is provided by the observation of an exponential yield increase in the range hν=3–4 eV, as evident from Fig. 2 (open symbols for positive bias). This observation suggests that electrons need to tunnel through some barrier to enter the CB of Al_2O_3. Consistent with this hypothesis is that the IPE yield increases exponentially with electric field as well, as both the barrier height and the field enter together into the tunneling exponent [see, e.g., Eq. (1) in Ref. 15 or the Fowler–Nordheim expression].

To determine interface energy barriers, the spectral thresholds were plotted as a function of the square root of the average electric field in the oxide stack (the Schottky plot). The field was calculated by subtracting the built-in voltage, at which the IPE current appears, from the applied bias to account for the metal-InP work function difference, and then dividing the obtained value by the oxide thickness estimated from TEM images. The results, compiled for all studied samples in Fig. 4(a), clearly show that the threshold Φ_1 is barely sensitive to the initial InP surface preparation and, therefore, can be associated with direct IPE into the CB of Al_2O_3. By contrast, the lower threshold Φ_2 is highly sensitive to the pre-ALD surface treatment and even to the conductivity type of the InP substrate allowing us to associate it with the IPE from InP into the CB of the IL. In Fig. 4(a) we also compare Φ_2 values obtained from the $Y^{1/3}$-hν plot (■) to those obtained from the *log* plot shown in Fig. 2 by extrapolating the yield to the sub-threshold background level (small filled squares).

Extrapolation to zero field gives consistent results with average values $\Phi_1^0=4.05\pm0.10$ eV and $\Phi_2^0=3.70\pm0.15$ eV, thus even when using different threshold

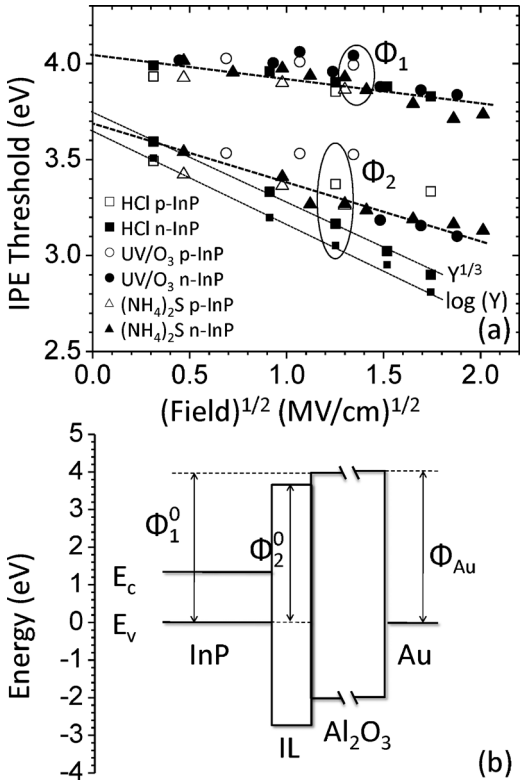


FIG. 4. (a) Schottky plot of the field dependent IPE thresholds measured for differently prepared InP/Al_2O_3 interfaces. For the n-InP/Al_2O_3 sample with pre-ALD HCl treatment the values of the lower barrier Φ_2 obtained from the log(Y)-hν (Fig. 2) and $Y^{1/3}$-hν (Fig. 3) plots are shown by small and large filled squares, respectively. Lines illustrate the determination of average zero-field barrier heights Φ_1^0 and Φ_2^0 between the top of the InP VB and the CB bottom of Al_2O_3 and of the IL, respectively; (b) Energy band diagram of the InP/Al_2O_3/Au structure inferred from the measured barrier values. The origin of the energy scale is at the top of the InP valence band.

determination plots for Φ_2. With these values together with the band gap width of the IL and Al_2O_3, and the measured barrier between the Fermi level of Au and the Al_2O_3 CB, we arrive at the electron band diagram shown in Fig. 4(b). The CB offsets can be estimated by subtracting the known band gap of InP (1.35 eV at 300 K) from the measured barriers: $\Delta E_c(\mathrm{InP}/\mathrm{Al_2O_3}) = 2.7 \pm 0.10$ eV and $\Delta E_c(\mathrm{InP}/\mathrm{IL}) = 2.35 \pm 0.15$ eV. Here, we note that the former offset nearly coincides with the theoretical prediction,[16] while the second one complies with the offset estimated for the InP/$In(PO_3)_3$ interface.[17] Apparently then, the P-rich IL may be associated with $In(PO_3)_3$ as the inferred IL band gap width of 6.5 eV is close to the 6.9 eV gap of $In(PO_3)_3$ layers grown on InP.[17,18]

The above results suggest that, similarly to the previously studied interfaces of arsenides,[6–8] the IL plays an important role in electron injection processes as it provides the lowest barrier for electrons in InP. Potentially, oxidation of InP may result in oxides with an even narrower gap than that of $In(PO_3)_3$: In $InPO_4$ the gap narrows to 4.5 eV (Ref. 19) and even to 3.5 eV in anodic oxide on InP.[20] These narrow-gap phases may further reduce the IL-related barrier potentially explaining the anomalously strong field-induced barrier lowering in some samples as demonstrated (Φ_2) in Fig. 4(a). Moreover, we found that at the (100)InP/ALD HfO_2 interface the spectral threshold of electron IPE only slightly exceeds 2 eV (spectra not shown). This is likely caused by In-rich IL formation and may explain the recently reported charge instability of InP/HfO_2 interfaces.[21]

In conclusion, we found that ALD Al_2O_3 provides a high CB offset, of 2.7 eV, with (100)InP. However, it is also observed that the formation of an IL due to oxidation of semiconductor may reduce the barrier height for electrons significantly, particularly if a high electric field is applied [cf. Fig. 4(a)]. To avoid this undesirable effect, the concentration of indium in the IL should be reduced; According to the results P-rich oxide on InP provides a sufficiently large CB offset in excess of 2 eV.

PH acknowledges the financial support of Science Foundation Ireland under Grant No. SFI/09/IN.1/I2633.

[1] Y. Q. Wu, Y. Xuan, T. Shen, P. D. Ye, Z. Cheng, and A. Lochefeld, Appl. Phys. Lett. **91**, 022108 (2007).
[2] H. Zhao, D. Shahrjerdi, F. Zhu, M. Zhang, H.-S. Kim, I. Ok, J. H. Yum, S. I. Park, S. K. Banerjee, and J. C. Lee, Appl. Phys. Lett. **92**, 233508 (2008).
[3] H. Zhao, Y.-T. Chen, J. H. Yum, Y. Wang, N. Goel, and J. C. Lee, Appl. Phys. Lett. **94**, 193502 (2009).
[4] H. Zhao, Y.-T. Chen, J. H. Yum, Y. Wang, F. Zhou, F. Xue, and J. C. Lee, Appl. Phys. Lett. **96**, 102101 (2010).
[5] N. V. Nguyen, O. A. Kirillov, W. Jiang, W. Wang, J. S. Suehle, P. D. Ye, Y. Xuan, N. Goel, K. W. Choi, W. Tsai, and S. Sayan, Appl. Phys. Lett. **93**, 082105 (2008).
[6] V. V. Afanas'ev, M. Badylevich, A. Stesmans, G. Brammertz, A. Delabie, S. Sionke, A. O'Mahony, I. M. Povey, M. E. Pemble, E. O'Connor, P. K. Hurley, and S. B. Newcomb, Appl. Phys. Lett. **93**, 212104 (2008).
[7] V. V. Afanas'ev, A. Stesmans, G. Brammertz, A. Delabie, S. Sionke, A. O'Mahony, I. M. Povey, M. E. Pemble, E. O'Connor, P. K. Hurley, and S. B. Newcomb, Appl. Phys. Lett. **94**, 202110 (2009).
[8] N. V. Nguyen, M. Xu, O. A. Kirillov, P. D. Ye, C. Wang, K. Cheung, and J. S. Suehle, Appl. Phys. Lett. **96**, 052107 (2010).
[9] S. J. Pennycook, Ultramicroscopy **30**, 58 (1989).
[10] D. B. Williams and C. B. Carter, *Transmission Electron Microscopy* (Plenum, New York, 1996), p. 353.
[11] V. V. Afanas'ev and A. Stesmans, J. Appl. Phys. **102**, 081301 (2007).
[12] V. I. Gavrilenko, A. M. Grekhov, D. V. Korbutyak, and V. G. Litovchenko, *Optical Properties of Semiconductors* (Naukova Dumka, Kiev, 1987).
[13] V. V. Afanas'ev, M. Houssa, A. Stesmans, and M. M. Heyns, J. Appl. Phys. **91**, 3079 (2002).
[14] R. J. Powell, J. Appl. Phys. **41**, 2424 (1970).
[15] G. B. Alers, K. S. Krisch, D. Monroe, B. E. Weir, and A. M. Chang, Appl. Phys. Lett. **69**, 2885 (1996).
[16] J. Robertson and B. Falabretti, J. Appl. Phys. **100**, 014111 (2006).
[17] Y. Robach, M. P. Besland, J. Joseph, G. Hollinger, P. Viktorovitch, P. Ferret, M. Pitavel, A. Falcou, and G. Post, J. Appl. Phys. **71**, 2981 (1992).
[18] G. Lévêque and Y. Villachon-Renard, Appl. Opt. **29**, 3207 (1990).
[19] J. F. Wager, C. W. Wilmsen, and L. L. Kazmerski, Appl. Phys. Lett. **42**, 589 (1983).
[20] A. A. Studna and G. L. Gualtieri, Appl. Phys. Lett. **39**, 965 (1981).
[21] Y.-T. Chen, H. Zhao, Y. Wang, F. Xue, F. Zhou, and J. C. Lee, Appl. Phys. Lett. **96**, 253502 (2010).